Minimizing Pedicle Screw Pullout Risks: A Detailed Biomechanical Analysis of Screw Design and Placement

Rohan-Jean Bianco, Pierre-Jean Arnoux, Eric Wagnac, Jean-Marc Mac-Thiong, Carl-Eric Aubin

▶ **To cite this version:**

Rohan-Jean Bianco, Pierre-Jean Arnoux, Eric Wagnac, Jean-Marc Mac-Thiong, Carl-Eric Aubin. Minimizing Pedicle Screw Pullout Risks: A Detailed Biomechanical Analysis of Screw Design and Placement. Clinical Spine Surgery, 2016, 31p. 10.1097/BSD.0000000000000151 . hal-01472882v2

HAL Id: hal-01472882
https://hal.science/hal-01472882v2

Submitted on 21 Feb 2017

HAL is a multi-disciplinary open access archive for the deposit and dissemination of scientific research documents, whether they are published or not. The documents may come from teaching and research institutions in France or abroad, or from public or private research centers.

L'archive ouverte pluridisciplinaire **HAL**, est destinée au dépôt et à la diffusion de documents scientifiques de niveau recherche, publiés ou non, émanant des établissements d'enseignement et de recherche français ou étrangers, des laboratoires publics ou privés.

Journal of Spinal Disorders and Techniques Publish Ahead of Print
DOI:10.1097/BSD.0000000000000151

Manuscript to be submitted to Journal of Spinal Disorders & Techniques

TITLE:

Minimizing pedicle screw pullout risks: a detailed biomechanical analysis of screw design and placement.

Rohan-Jean Bianco [a,b,c], Pierre-Jean Arnoux [c] Ph.D., Eric Wagnac [a,c] Eng., Ph.D., Jean-Marc Mac-Thiong [b,d,e] M.D., Ph.D. and Carl-Éric Aubin [a,b,d] Ph.D., P.Eng.

(a) Department of Mechanical Engineering, Polytechnique Montréal, P.O. Box 6079, Downtown Station, Montreal (Quebec), Canada H3C 3A7

(b) Sainte-Justine University Hospital Center, 3175, Cote Sainte-Catherine Road, Montreal (Quebec), Canada H3T 1C5

(c) Laboratoire de Biomécanique Appliquée, UMRT24 IFSTTAR/Aix-Marseille Université, Boulevard Pierre Dramard, 13916 Marseille Cedex 20, France

(d) Department of Surgery, Université de Montréal, 2900 Boulevard Edouard-Montpetit, Montreal, (Quebec), Canada H3T 1J4

(e) Department of Surgery, Hôpital du Sacré-Cœur de Montréal, 5400, boul. Gouin Ouest Montréal (Québec), Canada H4J 1C5

Address for notification, correspondence and reprints:

Copyright © Lippincott Williams & Wilkins. Unauthorized reproduction of the article is prohibited.

ACCEPTED

Carl-Éric Aubin, Ph.D., P.Eng.

Full Professor

NSERC/Medtronic Industrial Research Chair in Spine Biomechanics

Polytechnique Montreal, Department of Mechanical Engineering

P.O. Box 6079, Downtown Station, Montreal (Quebec), H3C 3A7 CANADA

E-mail: carl-eric.aubin@polymtl.ca

Phone: 1 (514) 340-4711 ext. 2836; Fax: 1 (514) 340-5867

ACKNOWLEDGEMENTS:

Funded by the Natural Sciences and Engineering Research Council of Canada (Industrial Research Chair with Medtronic of Canada).

CONFLICT OF INTEREST STATEMENT:

Authors have not received any payment for conducting this work and are in no conflict of interest.

Manuscript to be submitted to Journal of Spinal Disorders & Techniques

TITLE:

Minimizing pedicle screw pullout risks: a detailed biomechanical analysis of screw design and placement.

Abstract word count: 263

Main text word count: 3223

Number of tables: 1

Number of figures: 6

ACCEPTED

Copyright © Lippincott Williams & Wilkins. Unauthorized reproduction of the article is prohibited.

ABSTRACT

Study design: Detailed biomechanical analysis of the anchorage performance provided by different pedicle screw design and placement strategies under pullout loading.

Objective: To biomechanically characterize the specific effects of surgeon-specific pedicle screw design parameters on anchorage performance using a finite element model (FEM).

Summary of background data: Pedicle screw fixation is commonly used in the treatment of spinal pathologies. However, there is little consensus on the selection of an optimal screw type, size, and insertion trajectory depending on vertebra dimension and shape.

Methods: Different screw diameters and lengths, threads and insertion trajectories were computationally tested using a design of experiment (DOE) approach. A detailed FEM of an L3 vertebra was created including elastoplastic bone properties and contact interactions with the screws. Loads and boundary conditions were applied to the screws to simulate axial pullout tests. Force-displacement responses and internal stresses were analyzed to determine the specific effects of each parameter.

Results: The DOE analysis revealed significant effects ($p<0.01$) for all tested principal parameters along with the interactions between diameter and trajectory. Screw diameter had the greatest impact on anchorage performance. The best insertion trajectory to resist pullout involved placing the screw threads closer to the pedicle walls using the straight-forward insertion technique, which showed the importance of the cortical layer grip. The simulated

Copyright © Lippincott Williams & Wilkins. Unauthorized reproduction of the article is prohibited.

ACCEPTED

cylindrical single-lead thread screws presented better biomechanical anchorage than the conical dual-lead thread screws in axial loading conditions.

Conclusions: The model made it possible to quantitatively measure the effects of both screw design characteristics and surgical choices, enabling to recommend strategies to improve single pedicle screw performance under axial loading.

KEYWORDS:

Finite Element Analysis, Pedicle Screw, Pullout Test, Spinal Instrumentation

ACCEPTED

Copyright © Lippincott Williams & Wilkins. Unauthorized reproduction of the article is prohibited.

INTRODUCTION

Pedicle screw fixation is commonly used in spinal instrumentation surgeries to connect rods to vertebrae in order to correct spine alignment, stabilize vertebrae and reach an arthrodesis [1]. To be effective, the pedicle screw constructs must withstand intra-operative loading as well as physiological forces due to daily post-operative activities.

In current practice, numerous screw designs (various screw shaft threads and shape, screw heads articulated with the screw shaft, materials), insertion and manipulation techniques afford the surgeon many options. However, there is little consensus on the selection of an optimal type of screw, size, and trajectory (insertion point, tapping and screw alignment) depending on vertebra dimension and shape and bone mechanical properties. These choices are determined at the discretion of the surgeon based on his/her experience and practice [2, 3]. Computer-assisted surgery systems guide surgeons, in real-time, to properly insert the screws through the pedicles [4], but the insertion strategy itself, generally, remains empirical.

In vitro experiments, such as axial pullout tests, provide significant insight into the biomechanics of screw-bone interactions and failure forces. Several surgical parameters have been studied such as the trajectory and entry point [5]. However, experimentations reveal limitations in terms of inter-individual variability (bone density, pedicle morphology, etc.) and reproducibility. Also, the surgical techniques used during those tests can significantly affect mechanical strength [6].

Such limitations in determining the optimal parameters for obtaining strong pedicle screw fixation could be overcome by finite element analysis [7]. A few finite element models (FEM)

Copyright © Lippincott Williams & Wilkins. Unauthorized reproduction of the article is prohibited.

ACCEPTED

have been developed, but most fail to take into account local geometric details and advanced mechanical properties such as plastic deformation, bone fracture, material properties distribution and contact friction at the bone-screw interface. Previous models focused either on detailed pedicle models [8] or on simplified complete vertebra models [9], which did not permit studying the detailed effects of every screw design parameter and insertion trajectory individually or combined simultaneously.

The objective of this study was to analyze the bone-screw mechanical interaction and test several parameters such as the pedicle screw size, thread design, insertion point and trajectory that could minimize the risk of instrumentation failure using a detailed FEM of an instrumented vertebra.

ACCEPTED

Copyright © Lippincott Williams & Wilkins. Unauthorized reproduction of the article is prohibited.

MATERIALS AND METHODS

For this study, two different existing multi-axial screws were used with different thread patterns (Figure 2) from the CD Horizon spinal systems (Medtronic Inc., Memphis, USA). The first screw (CD HORIZON® LEGACY™ screw) was a cylindrical equally spaced single-lead thread screw, while the second (CD HORIZON® OSTEOGRIP™ screw) had a slightly conical inner core and the pitch of the distal part was dual-lead thread (double pitch in the pedicle region). In addition, the single-lead thread screw crests were thicker and had spherical bases, while the dual-lead thread screw crests were thinner and had conical bases.

Two different screw lengths (40mm - 50mm) and screw diameters (6.5mm - 8.5mm) were tested. The screws were virtually positioned and placed through the pedicle following the free hand localization technique, which used anatomical landmarks on vertebrae during an open surgery [10]. The entry point was enlarged by removal of the superficial cortical elements simulating the use of a bone rongeur or a burr [11]. The screw tapping was modeled using a boolean operation method to remove bone at the future location of the screw. Two common trajectories (anatomic (AN) and straight forward (SF) [2, 3]) were tested for each screw (Figure 2).

A design of experiment (DOE) was performed in order to biomechanically investigate both the individual and combined effects of the thread type, lengths, diameters and insertion trajectories on the fixation strength of the pedicle screws. Each parameter had two extreme values, as described above. A DOE is a statistical method enabling to determine if there is a statistically significant effect that a particular factor exerts on the dependent variables of

Copyright © Lippincott Williams & Wilkins. Unauthorized reproduction of the article is prohibited.

interest [12]. The DOE was based on a Box, Hunter and Hunter full plan with four factors leading to 16 runs. The statistical analysis was performed using Statistica 8 (StatSoft, Inc., Tulsa, USA). Due to the determinist aspect of FEM simulations an alpha acceptance of less than 0.01 was chosen for significance.

The geometry used for the FEM was built from CT-scan images of a L3 vertebra (contiguous slices of 0.6 mm thick) of a 50th percentile human volunteer (European, 32 years old, 75 kg, 1,75 m) with no known spinal pathology to obtain a "generic shape". The vertebra (Figure 1) was modeled by taking into account the separation of the trabecular and cortical bone with realistic regional thickness from morphologic measurements [13, 14]. The pedicles were 13 mm in height and 11 mm in width, while the cortical bone thickness varied from 1.0 to 1.5 mm. The vertebra FEM was meshed with four node tetrahedral elements of 0.5 mm characteristic length in the peri-implant region (region of interest) and 1 mm characteristic length in the farter regions. The mesh distribution was refined through a convergence study to adapt to the region of interest and minimize the number of nodes to satisfactorily balance accuracy and computer resources. The screws external surface was modeled as a shell with characteristic triangular elements of 0.5 mm. The triangle-based elements were chosen for their ability to comply with complex geometry and their non-warpage properties. The model as a whole contained ~50 000 nodes (~250 000 elements).

Rigid body properties were applied to some node groups of the model away from the region of interest and to all nodes of the screw, thus reducing computational time. The screw was considered rigid due to the high material property gradient at the interface, which was several times higher than the bone. These assumptions were verified to have marginal impact on the results. The bone/screw interface was modeled using a point/surface penalty method for the

Copyright © Lippincott Williams & Wilkins. Unauthorized reproduction of the article is prohibited.

ACCEPTED

contact interface with a Coulomb type friction coefficient of 0.2 [15] and minimal gap of 0.05 mm.

The cortical and trabecular bones were considered as homogeneous isotropic materials. Their properties were estimated from a previous study using an inverse finite element method based upon experimental tests performed on fresh post-mortem elderly human subjects [16]. The model integrates an elastoplastic material law (Johnson-Cook) to simulate bone failure (Table 1) [17]. Thus, before plastic deformation occurs (equivalent stress < yield stress), the material behaves as linear elastic. During plastic deformation, the equivalent stress was computed using the relation $\sigma = a + b\ \varepsilon_p^n$, where σ = equivalent stress, a = yield stress, b = hardening modulus, ε_p= plastic strain (true strain), and n = hardening exponent. Once the failure plastic strain (ε_{max}) of a given element locally was reached, failure occurred and the corresponding element deleted, thus simulating the bone fracture.

Boundary and loading conditions were applied in order to simulate screw pullout as described in the ASTM-F543 standard [18]. This specific test was performed to assess the biomechanical strength of the screw anchorage by applying a ramped axial tensile force to the screw until total pullout. The external nodes of the anterior part of the vertebral body were fixed to simulate rigid embedment. In addition, a constraining slide link condition was applied to the whole screw (leaving only the translation in the screw axis free) to simulate the effect of fixation with the loading shaft and avoid any off axis displacement.

The simulations were performed using the explicit dynamic FEM solver RADIOSS v5.1 (Altair Engineering inc., Troy, USA) with a kinetic relaxation scheme to perform a quasi-static analysis. The stresses along the screw threads during the pullout were analyzed. The

Copyright © Lippincott Williams & Wilkins. Unauthorized reproduction of the article is prohibited.

ACCEPTED

initial stiffness and the peak pullout force extracted from the computed load-displacement curve were compared with available previously published experimental data [19-22] for model validation.

ACCEPTED

Copyright © Lippincott Williams & Wilkins. Unauthorized reproduction of the article is prohibited.

RESULTS

The computed load-displacement curves exhibited a non-linear behavior (Figure 3), which could be divided into three zones. In the first part of the curve (zone A), the bone-screw construct followed a linear elastic stiffness slope, without bone damage or failure. Once yield strength was reached (zone B), bone element failure commenced at the local level in the peri-implant area and plastic deformation occurred. The stiffness decreased as plastic strain failure was reached on bone elements, which contributed to an eventual total loss of bone-screw stiffness. Screw failure occurred at the end of zone B at the level of the peak pullout force. Zone C showed a decrease in stiffness and pullout force until the screw was totally pulled out of the bone.

Compared to previously published data, the simulated initial stiffness' (1327 $N.mm^{-1}$ – 4800 $N.mm^{-1}$) were slightly higher than that obtained experimentally on human cadaveric vertebrae (1100$N.mm^{-1}$ – 2700 $N.mm^{-1}$) [5], while the simulated peak pullout forces (220 N – 750 N) were within the published range (218 – 840 N) [5]. The discrepancy between the experimental values can be explained by the natural variability of human subjects (due to age and bone quality, vertebra size and level), the difference in screw design, and also by the poor reproducibility of such experiments [21, 23].

In the bone structure, the Von Mises stress distribution revealed high stresses at each thread, most pronounced at the tip of the screw and in the pedicle isthmus area. The overall fracture pattern initiated in the trabecular bone, around the screw tip, and propagated to the head of the screw until total pullout. Differences in the stress distribution pattern between the two thread

Copyright © Lippincott Williams & Wilkins. Unauthorized reproduction of the article is prohibited.

ACCEPTED

profiles were observed (Figure 4). The cylindrical single-lead thread screw revealed an even bone stress distribution from tip to head, with higher stress reported at the tip of the screw and in the pedicle isthmus area. At the same pullout force, the conical dual-lead thread screw showed an irregular stress distribution with several stress concentration zones at each thread of the trabecular section distally.

The DOE analysis revealed significant effects ($P<0.01$) for all tested major factors (i.e. the type, diameter, length and trajectory of the screw) on both of the indices studied (Figure 5). Screw diameter consistently had the highest effect on anchorage strength. Pareto charts report the effects of the tested design parameters, ordered in rank of importance using the "t values". Looking at peak pullout force response, the significant effects in descending order included screw diameter, insertion trajectory, thread type and screw length. The resulting initial stiffness and peak pullout force were highly correlated ($r^2=0.84$), thus showing that one is a good indicator of the other.

The study of the interaction between individual parameters showed significant effects for screw trajectory combined with thread type and screw trajectory combined with diameter. The anatomic trajectory allowed larger diameter screws to be placed, in addition to longer screws (Figure 5). Other combinations of factors did not reveal significant effects, as their effects were only linear predictions of the individual variables.

The response distribution box plots (Figure 6) indicated that the highest initial stiffness' and peak pullout forces were obtained when the screw was longer (50 mm) and with a larger diameter (8.5 mm). The Straight Forward trajectory exhibited better biomechanical anchorage

Copyright © Lippincott Williams & Wilkins. Unauthorized reproduction of the article is prohibited.

ACCEPTED

than the Anatomic trajectory. Better anchorages were obtained with the cylindrical single-lead thread screw than the dual-lead thread screw with the slightly conical diameter.

DISCUSSION

Screw diameter had the greatest impact on anchorage performances, which is consistent with previous biomechanical studies showing that a screw's major diameter determines pullout strength [24]. The major diameter is directly related to crest height, thus to the contact surface with the bone, leading to better anchorage. Furthermore, the increase of screw diameter in the isthmus of the pedicle leads to a closer connection with the cortical (harder) bone. For instance, a few crests of the 8.5mm screw were gripping the cortical bone in the pedicle region (without cortical wall violation). The pedicle fill could have been another index of interest in addition to the pedicle diameter but a single vertebra only was used in this study; therefore the filling ratio would be quite the same.

At a given size, the dual thread screw had a reduced anchorage capability as compared to the single thread screw. This could be explained by the crest design and height, which are different for the same major diameter. The single-lead thread screw type has a spherical and even thread base contrary to the dual-lead thread screw type, which has a spherical thread base in the pedicle region and a conical thread base in the trabecular region. The effect of these designs resulted in different stress distribution and concentration spots for each type of screw (Figure 4). The stress concentration spots near the distal threads in the dual thread screw design lead to an earlier bone fracture, thus weaker anchorage of the dual-lead thread screw. However, the simulated bone fracture occurred at a high force level (500N-600N), such that any difference should not be an issue during "normal" intra-operative correction

Copyright © Lippincott Williams & Wilkins. Unauthorized reproduction of the article is prohibited.

maneuvers or post-operative functional loads, but could be a problem in the case of excessive loads [25]. This study focused only on axial forces; no conclusion could be made on the different loads as could be applied to screw intra- or post-operatively.

The screw profile (conical vs. cylindrical) also has an influence on screw performance, as inferred by the work of Abshire et al., 2001 and Hsu et al., 2005 who determined that conical screws and dual-lead thread screws improve the insertion torque. It seems intuitive that a higher insertion torque is correlated to higher peak pullout force [24, 26], however it has been demonstrated that insertion torque is not a good predictor of pullout force as the relations are screw and geometry specific [27, 28]. The results of the current study, revealed a reduced performance when using a screw with a conical profile. It is important to note that this factor was dependent on the thread type, meaning the results are a combination of both the screw profile and thread type.

The screw insertion process is generally preceded by a pre-tapping step using a smaller diameter than the screw. This study did not take into account the effect of pressfit and pedicle deformation [29] during screw insertion, which has an effect on screw anchorage [30]. This initial stress state might have an impact if other insertion techniques are investigated, particularly related to the tapping process. Further work is needed to understand the influence of the screw insertion in order to implement the stress and bone deformation.

The screw diameters used for this current study were larger than those generally used during corrective surgeries. The larger screws were chosen to accommodate the pedicle size of the model. To complete this investigation, further studies with a wider variety of lengths and diameters and vertebrae types should be performed.

Copyright © Lippincott Williams & Wilkins. Unauthorized reproduction of the article is prohibited.

ACCEPTED

The SF trajectory leads the screw threads closer to the cortical wall, which could explain the increased stiffness and pullout force resulting in better anchorage. As the cortical bone layer has a major effect on screw anchorage [22], its interaction with the screw trajectory and diameter is particularly important.

The simulated fracture patterns, beginning around the tip of the screw and propagating to the head, suggest that higher stresses occurred first in the areas around the tip and the pedicle isthmus. This result is contrary to predicted failure mechanisms from threaded assembly theory [31], which describes the higher stress area as the contact area around the three first inserted threads bearing 70% of the total load. The computed results showed a more uniform distribution of contact forces along the screw shaft with an increasing trend in the screw tip area. This discrepancy was also reported in other numerical studies on screw pullout in bone structures [32, 33], which agree with the reported results. Such a divergence could be explained by the material property gradient between bone and screw, but also by the differences in thread design between industrial and medical screws. The results suggest the threaded assembly theory, used for standard industrial screws, [31] may not be adequate for pedicle screw design anchored in bone.

The initial toe-region was not considered in this study as it represented a numerical effect of the contact interface definition. Although this phenomenon is observable in experimental curves, it only represents the early effects of loading and has no outlook on the biomechanical performance of the screws.

Even though the geometry used represents a "generic" vertebra shape, the material properties were derived from a finite element inverse method using lumbar vertebrae harvested from

Copyright © Lippincott Williams & Wilkins. Unauthorized reproduction of the article is prohibited.

ACCEPTED

elderly subjects (~ 70 years old). This is consistent with most reported experimental tests, mainly performed on elderly and osteoporotic vertebrae [19-22].

The bone material properties used in the model resulted from a finite element inverse method of slow dynamic compression tests [16], which may explain the higher stiffness values that were numerically obtained. The conditions of mechanical property extraction (axial compression) were different from the conditions described in this study; however it was assumed that the bone properties were isotropic. This assumption might lead to higher anchorage because bone properties have lower Young's modulus in the transverse directions than in the axial direction [34]. Furthermore, the model was intended to be used for relative comparisons and not as an absolute prediction tool, thus diminishing any numerical-experimental disparity issues.

The elasto-plastic material law (Johnson-Cook) used in this study assumes that the bony structures are isotropic and have a homogeneous distribution. In reality, the pedicle and the vertebral body have a complex and irregular bone distribution [13, 14, 35] leading to anisotropic properties. Further investigations, implementing heterogeneity in bone properties could be an alternative to investigate such effects. Alternative methods to model more accurately the complex internal bone structures such as micro Finite Element Analysis [33] or Smoothed Particle Hydrodynamics (SPH) exist, but require higher computational resources.

This study only focused on the behavior of individual screws under axial loading. Any effects on triangulation screw pairing or instrumentation assembly were not taken into account in the current study. The intended use of this model was to perform relative comparisons using a DOE approach, rather than absolute value analyses. The model created was extracted from a healthy man with no known spinal pathologies or deformities and the material properties were

Copyright © Lippincott Williams & Wilkins. Unauthorized reproduction of the article is prohibited.

ACCEPTED

considered as ideal (homogeneous and no osteoporosis). At this current state, no extrapolation should be made for deformed pedicles or osteoporotic vertebrae. Additional work would be required to modify this generic model to a more personalized one, in terms of geometry and material properties.

ACCEPTED

Copyright © Lippincott Williams & Wilkins. Unauthorized reproduction of the article is prohibited.

CONCLUSION

The design of experiment determined that the diameter of the screw had the highest impact on mechanical anchorage. The simulated cylindrical single-lead thread screws presented better biomechanical anchorage than the conical dual-lead thread screws in axial loading conditions. The trajectory promoting closer connection with the cortical bone provided a better mechanical anchorage.

A detailed and realistic FEM of an instrumented lumbar vertebra was developed to analyze and compare screw designs and trajectories. The developed comprehensive FEM is a valuable tool to analyze the pedicle screw biomechanics. It is a promising alternative to complex, expensive and specimen-specific in vitro experimental tests.

The recommendations provided can improve single screws performance under axial loading. Further studies should be undertaken to refine and fully validate this model, and to examine other types of loads as well as whole construct effects. The model could also be adapted to further analyze patient specific characteristics, such as osteoporotic or deformed vertebrae. Looking to the future, this ideology could lead to a computerized testing platform for new implant designs or as a surgery-planning tool to help clinicians.

ACCEPTED

Copyright © Lippincott Williams & Wilkins. Unauthorized reproduction of the article is prohibited.

REFERENCES:

1. Lenke LG, Kuklo TR, Ondra S, et al. Rationale behind the current state-of-the-art treatment of scoliosis (in the pedicle screw era). *Spine*, 2008. 33(10): p. 1051-1054.
2. Dhawan A, Klemme WR, and Polly DW, Jr. Thoracic pedicle screws: comparison of start points and trajectories. *Spine*, 2008. 33(24): p. 2675-2681.
3. Lehman RA, Jr., Polly DW, Jr., Kuklo TR, et al. Straight-forward versus anatomic trajectory technique of thoracic pedicle screw fixation: a biomechanical analysis. *Spine*, 2003. 28(18): p. 2058-2065.
4. Nottmeier EW, Seemer W, and Young PM. Placement of thoracolumbar pedicle screws using three-dimensional image guidance: experience in a large patient cohort. *Journal of Neurosurgery: Spine*, 2009. 10(1): p. 33-39.
5. !!! INVALID CITATION !!!
6. Brown BS, McIff TE, Glattes RC, et al. The effect of starting point placement technique on thoracic transverse process strength: an ex vivo biomechanical study. *Scoliosis*, 2010. 5:14.
7. Wagnac E, Michardiere D, Garo A, et al. Biomechanical analysis of pedicle screw placement: a feasibility study. *Studies in health technology and informatics*, 2010. 158: p. 167-171.
8. Zhang QH, Tan SH, and Chou SM. Effects of bone materials on the screw pull-out strength in human spine. *Medical engineering & physics*, 2006. 28(8): p. 795-801.
9. Chen CS, Chen WJ, Cheng CK, et al. Failure analysis of broken pedicle screws on spinal instrumentation. *Medical engineering and physics*, 2005. 27(6): p. 487-496.

ACCEPTED

Copyright © Lippincott Williams & Wilkins. Unauthorized reproduction of the article is prohibited.

10. Modi HN, Suh SW, Fernandez H, et al. Accuracy and safety of pedicle screw placement in neuromuscular scoliosis with free-hand technique. *European Spine Journal*, 2008. 17(12): p. 1686-1696.
11. Gaines RW, Jr. The use of pedicle-screw internal fixation for the operative treatment of spinal disorders. *Journal of Bone & Joint Surgery*, 2000. 82-A(10): p. 1458-1476.
12. Montgomery DC, *Design and analysis of experiments*. Vol. 7. 1997: Wiley New York.
13. Hirano T, Hasegawa K, Takahashi HE, et al. Structural characteristics of the pedicle and its role in screw stability. *Spine*, 1997. 22(21): p. 2504-2510.
14. Silva MJ, Wang C, Keaveny TM, et al. Direct and computed tomography thickness measurements of the human, lumbar vertebral shell and endplate. *Bone*, 1994. 15(4): p. 409-414.
15. Liu CL, Chen HH, Cheng CK, et al. Biomechanical evaluation of a new anterior spinal implant. *Clinical Biomechanics*, 1998. 13(1 Suppl 1): p. 40-45.
16. Garo A, Arnoux PJ, Wagnac E, et al. Calibration of the mechanical properties in a finite element model of a lumbar vertebra under dynamic compression up to failure. *Medical and Biological Engineering and Computing*, 2011. 49(12): p. 1371-1379.
17. El-Rich M, Arnoux PJ, Wagnac E, et al. Finite element investigation of the loading rate effect on the spinal load-sharing changes under impact conditions. *Journal of biomechanics*, 2009. 42(9): p. 1252-1262.
18. ASTM-F543, Standard Specification and Test Methods for Metallic Medical Bone Screws, 2009.
19. Abshire BB, McLain RF, Valdevit A, et al. Characteristics of pullout failure in conical and cylindrical pedicle screws after full insertion and back-out. *The Spine Journal*, 2001. 1(6): p. 408-414.

Copyright © Lippincott Williams & Wilkins. Unauthorized reproduction of the article is prohibited.

ACCEPTED

20. Inceoglu S, McLain RF, Cayli S, et al. Stress relaxation of bone significantly affects the pull-out behavior of pedicle screws. *Journal of Orthopaedic Research*, 2004. 22(6): p. 1243-1247.

21. Mehta H, Santos E, Ledonio C, et al. Biomechanical analysis of pedicle screw thread differential design in an osteoporotic cadaver model. *Clinical Biomechanics*, 2012. 27(3): p. 234-240.

22. Santoni BG, Hynes RA, McGilvray KC, et al. Cortical bone trajectory for lumbar pedicle screws. *The Spine Journal*, 2009. 9(5): p. 366-373.

23. Pfeiffer M, Gilbertson LG, Goel VK, et al. Effect of specimen fixation method on pullout tests of pedicle screws. *Spine*, 1996. 21(9): p. 1037-1044.

24. Cho W, Cho S, and Wu C. The biomechanics of pedicle screw-based instrumentation. *Journal of Bone & Joint Surgery*, 2010. 92(8): p. 1061-1065.

25. Wang X, Aubin CE, Labelle H, et al. Biomechanical Analysis of Corrective Forces in Spinal Instrumentation for Scoliosis Treatment. *Spine*, 2012: p. 1479-1487.

26. Kwok AWL, Finkelstein JA, Woodside T, et al. Insertional torque and pull-out strengths of conical and cylindrical pedicle screws in cadaveric bone. *Spine*, 1996. 21(21): p. 2429.

27. Inceoglu S, Ferrara L, and McLain RF. Pedicle screw fixation strength: pullout versus insertional torque. *The Spine Journal*, 2004. 4(5): p. 513-518.

28. Okuyama K, Abe E, Suzuki T, et al. Can insertional torque predict screw loosening and related failures? An in vivo study of pedicle screw fixation augmenting posterior lumbar interbody fusion. *Spine*, 2000. 25(7): p. 858-864.

29. Inceoglu S, Kilinçer C, Tami A, et al. Cortex of the pedicle of the vertebral arch. Part I: Deformation characteristics during screw insertion. *Journal of Neurosurgery: Spine*, 2007: p. 341-346.

Copyright © Lippincott Williams & Wilkins. Unauthorized reproduction of the article is prohibited.

ACCEPTED

30. Defino HLA. Study of the influence of the type of pilot hole preparation and tapping on pedicular screws fixation. *Acta Ortopedica Brasileira*, 2007. 15(4): p. 200-203.

31. Guillot J, *Assemblages par Elements Filetes Modelisations et Calcul*. Vol. B5560. 1987: Ed. Techniques de l'Ingénieur.

32. Chatzistergos PE, Magnissalis EA, and Kourkoulis SK. A parametric study of cylindrical pedicle screw design implications on the pullout performance using an experimentally validated finite-element model. *Medical engineering & physics*, 2010. 32(2): p. 145-154.

33. Wirth AJ, Müller R, and Harry van Lenthe G. The discrete nature of trabecular bone microarchitecture affects implant stability. *Journal of biomechanics*, 2012: p. 1060–1067.

34. Schmidt H, Heuer F, Drumm J, et al. Application of a calibration method provides more realistic results for a finite element model of a lumbar spinal segment. *Clinical Biomechanics*, 2007. 22(4): p. 377-384.

35. Defino HLA and Vendrame JR. Role of cortical and cancellous bone of the vertebral pedicle in implant fixation. *European Spine Journal*, 2001. 10(4): p. 325-333.

ACCEPTED

Copyright © Lippincott Williams & Wilkins. Unauthorized reproduction of the article is prohibited.

FIGURES:

Figure 1: Meshed L3 vertebra with a cylindrical single-lead thread screw (length 50mm, diameter 8.5 mm) inserted. Cortical regional thickness, elements used and mesh distribution shown. The bone was meshed with tetrahedral elements while the screw parts were meshed with triangular surfacic elements.

Figure 2: Multi-axial screws and screw trajectories superimposed on the vertebra shape. a) Cylindrical single-lead thread on top and dual-lead thread with doubled pitch in the pedicle region and the inner diameter is slightly conical below. b) In the sagittal plane (right view), the screws were parallel to the upper endplate of the vertebral body. In the transverse plane (left view), in the Straight Forward trajectory the screw was parallel to the sagittal plane of the vertebral body, while in the Anatomic trajectory the screw was inserted along the transverse orientation of the pedicle. The arrows show the direction of the pullout force applied.

Figure 3: Generic load-displacement curve from the simulated pullout test. The curve is divided in a first linear elastic zone (A), a second elasto-plastic zone with bone damage (B) and a third zone after the total pullout of the screw (C).

Figure 4: Peri-implant Von Mises stress distribution in the trabecular bone structure along the 6.5mm*50mm single-lead thread screw (top) and dual-lead thread screw (bottom) inserted in Straight Forward trajectory loaded with an axial force at 370N. Higher stress areas are observable around the screw tip and in the pedicle isthmus area (stress scale bars are at same level).

Copyright © Lippincott Williams & Wilkins. Unauthorized reproduction of the article is prohibited.

ACCEPTED

Figure 5: Pareto chart for the initial stiffness (a) and peak pullout force (b). The standardized effects estimates (absolute values) are plotted and classified in order of influence on the model in terms of "t value". Coupled effects are noted "a by b" where "a" and "b" are the factor denomination. Threshold level of significance was set at P = 0.01.

Figure 6: Box plot distribution of initial stiffness (top row) and peak pullout force (bottom row) for the 4 analyzed parameters: (1) type of screw; (2) screw diameter; (3) screw length; (4) screw trajectory. The best anchorage was obtained with the cylindrical single-lead thread screw of 8.5 mm diameter, 50 mm length with a Straight Forward trajectory.

ACCEPTED

Copyright © Lippincott Williams & Wilkins. Unauthorized reproduction of the article is prohibited.

TABLE:

Table 1: Material properties of the cortical and trabecular bone used in the FEM [16]

TABLE:

Table 1: Material properties of the cortical and trabecular bone used in the FEM [14]

Material properties	Cortical bone	Trabecular bone
Density (kg/mm^3)	2.0E-06	2.0E-7
Young modulus, *E* (MPa)	2625	48.75
Poisson ratio, *v*	0.3	0.25
Yield stress, *a* (MPa)	105	1.95
Hardening modulus, b (MPa)	875	16.3
Hardening exponent, n	1	1
Failure plastic strain, ε_{max}	0.04	0.04

ACCEPTED

Copyright © Lippincott Williams & Wilkins. Unauthorized reproduction of the article is prohibited.

Figure (TIF or EPS Only!!! Resolution of at least 300 dpi!)
Click here to download high resolution image

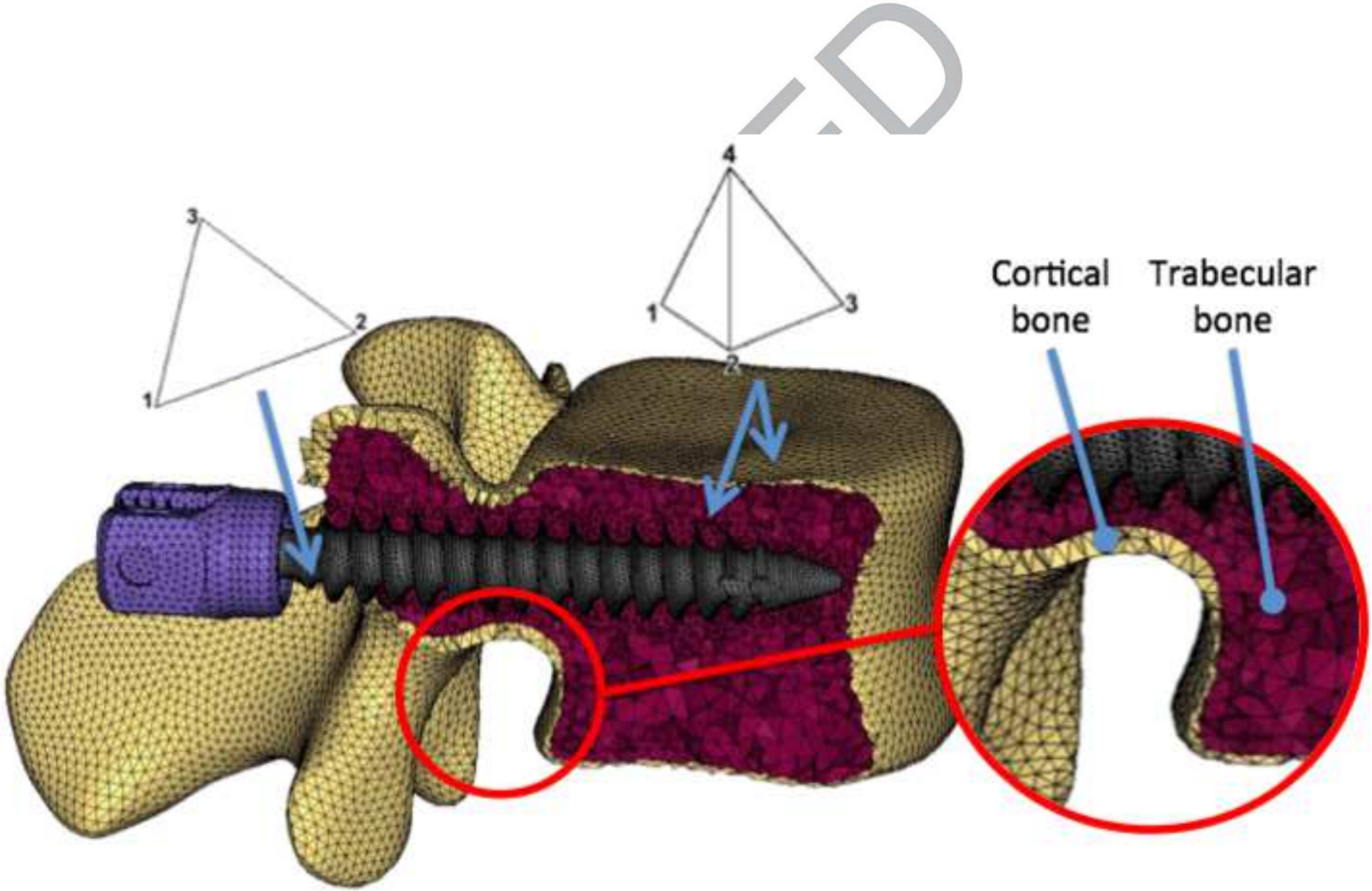

Copyright © Lippincott Williams & Wilkins. Unauthorized reproduction of the article is prohibited.

Figure (TIF or EPS Only!!! Resolution of at least 300 dpi!)
Click here to download high resolution image

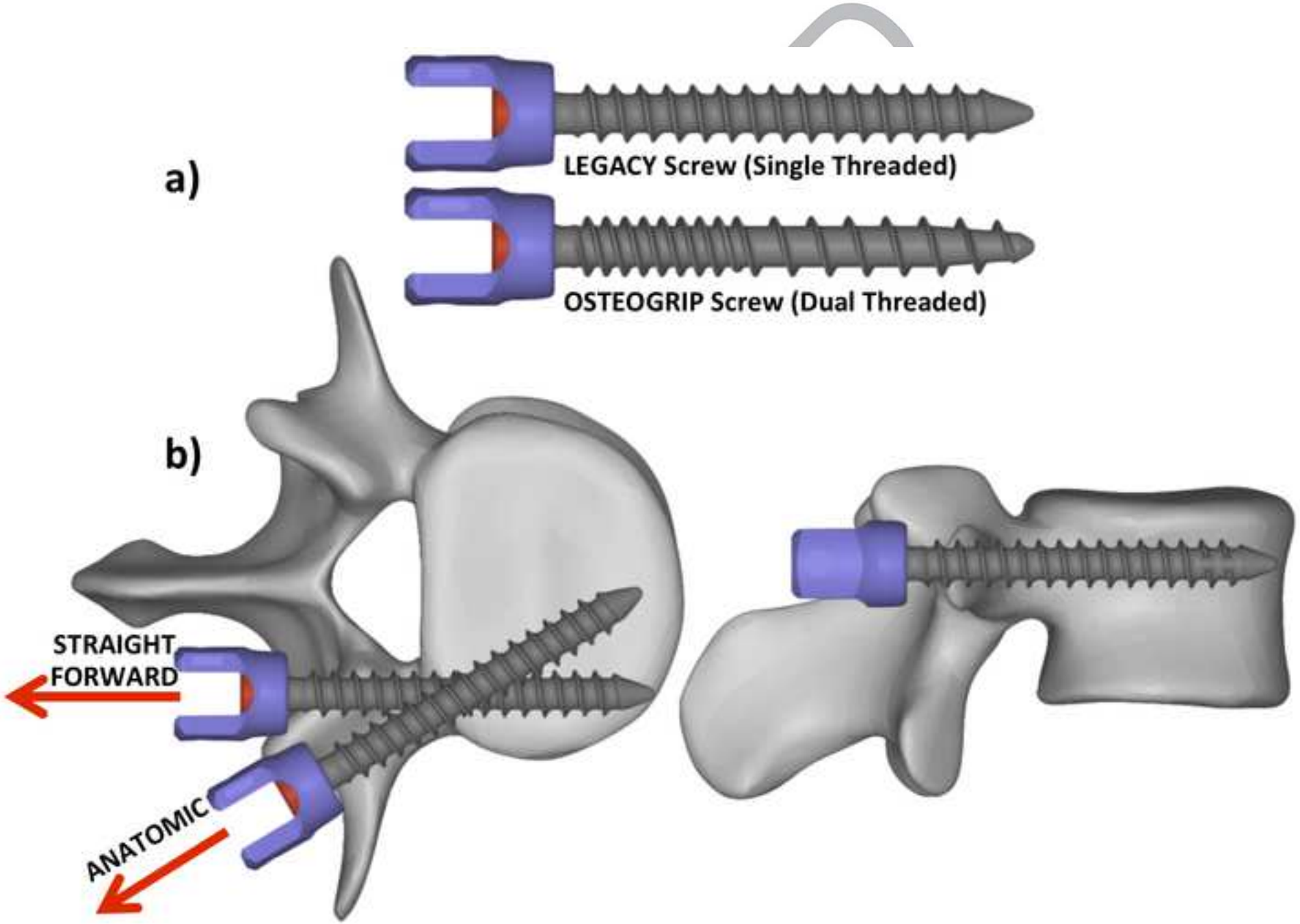

Copyright © Lippincott Williams & Wilkins. Unauthorized reproduction of the article is prohibited.

Figure (TIF or EPS Only!!! Resolution of at least 300 dpi!)
Click here to download high resolution image

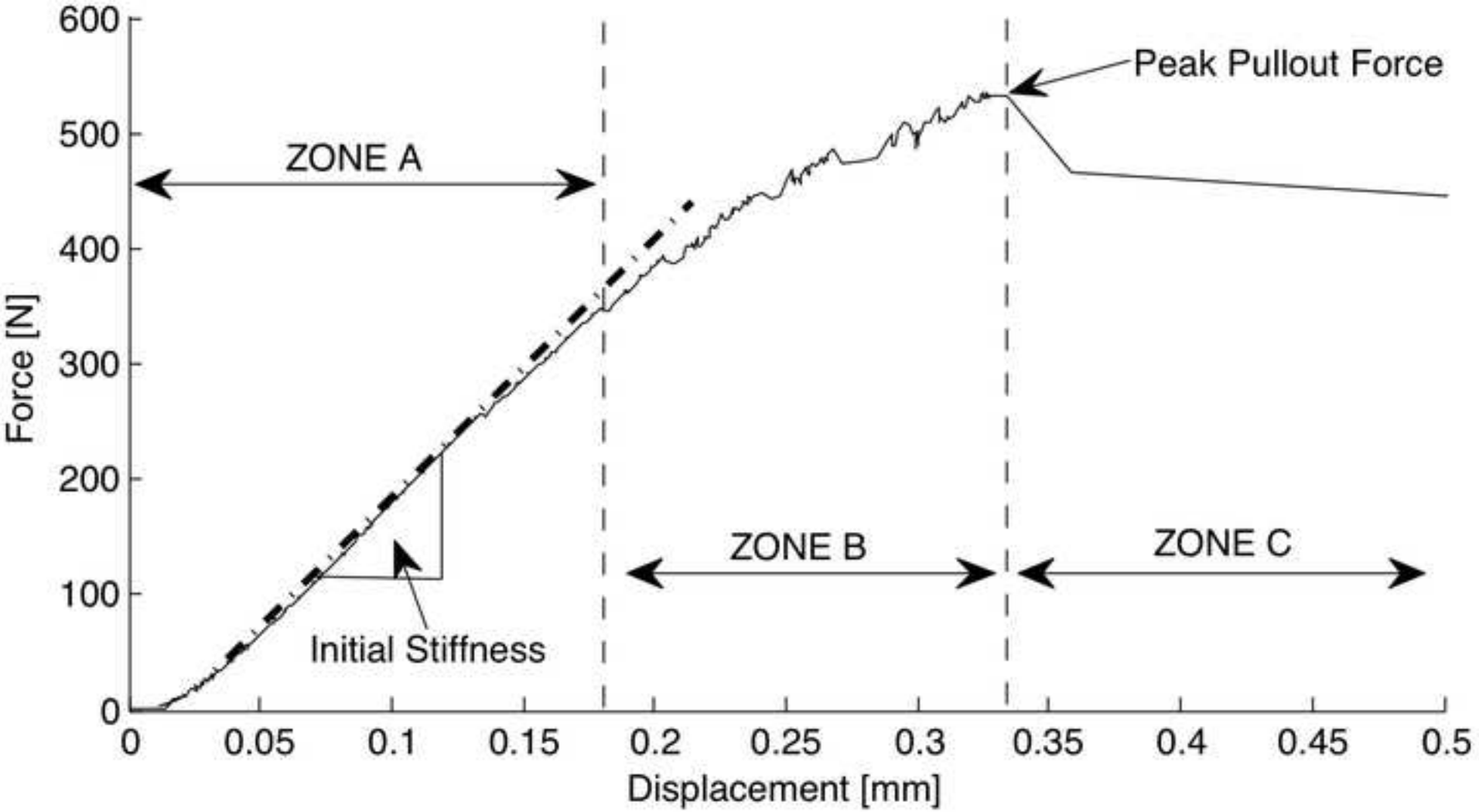

Copyright © Lippincott Williams & Wilkins. Unauthorized reproduction of the article is prohibited.

Figure (TIF or EPS Only!!! Resolution of at least 300 dpi!)
Click here to download high resolution image

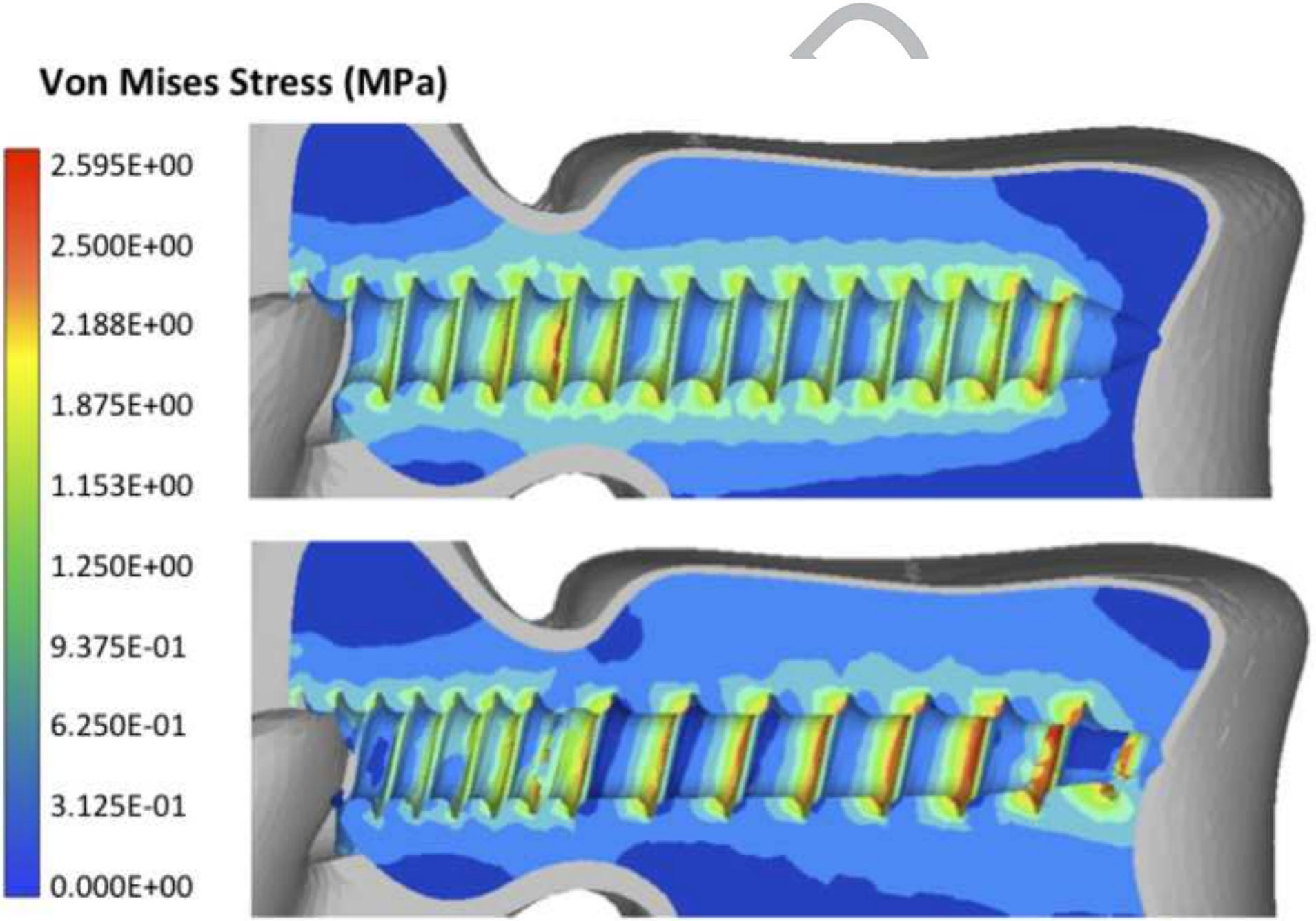

Copyright © Lippincott Williams & Wilkins. Unauthorized reproduction of the article is prohibited.

Figure (TIF or EPS Only!!! Resolution of at least 300 dpi!)
Click here to download high resolution image

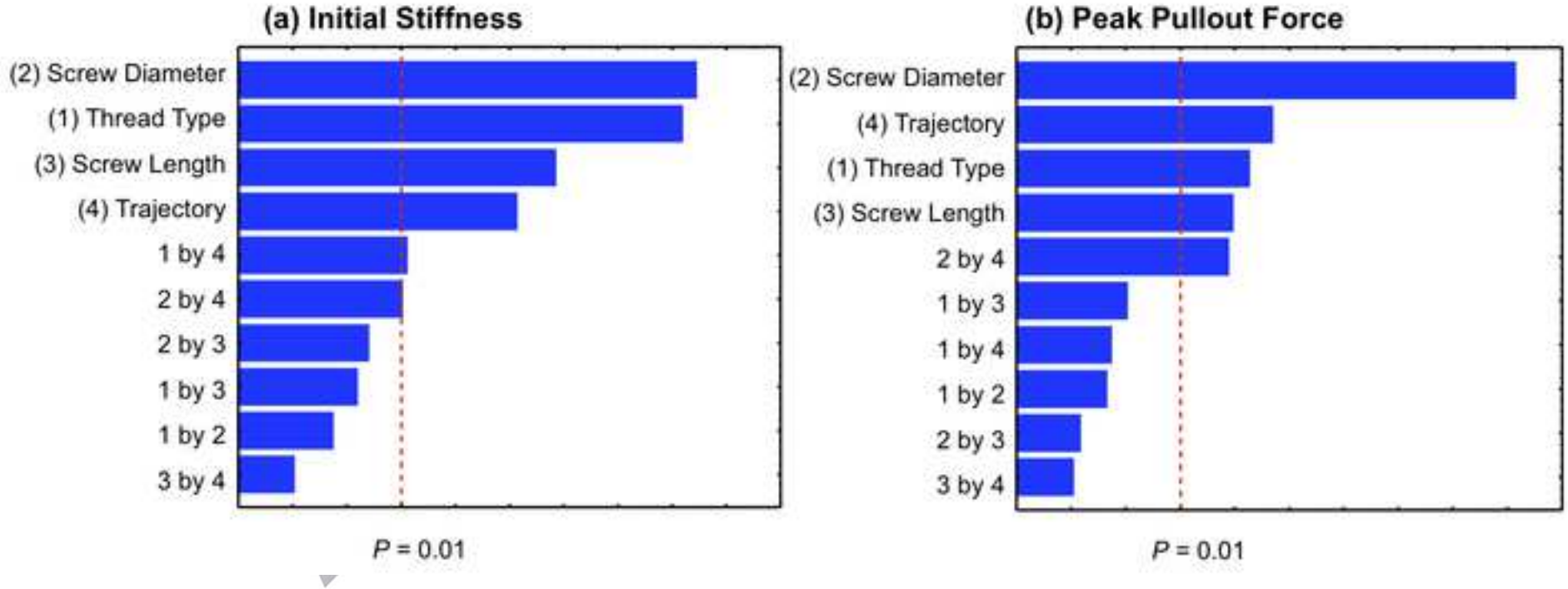

Copyright © Lippincott Williams & Wilkins. Unauthorized reproduction of the article is prohibited.

Figure (TIF or EPS Only!!! Resolution of at least 300 dpi!)
Click here to download high resolution image

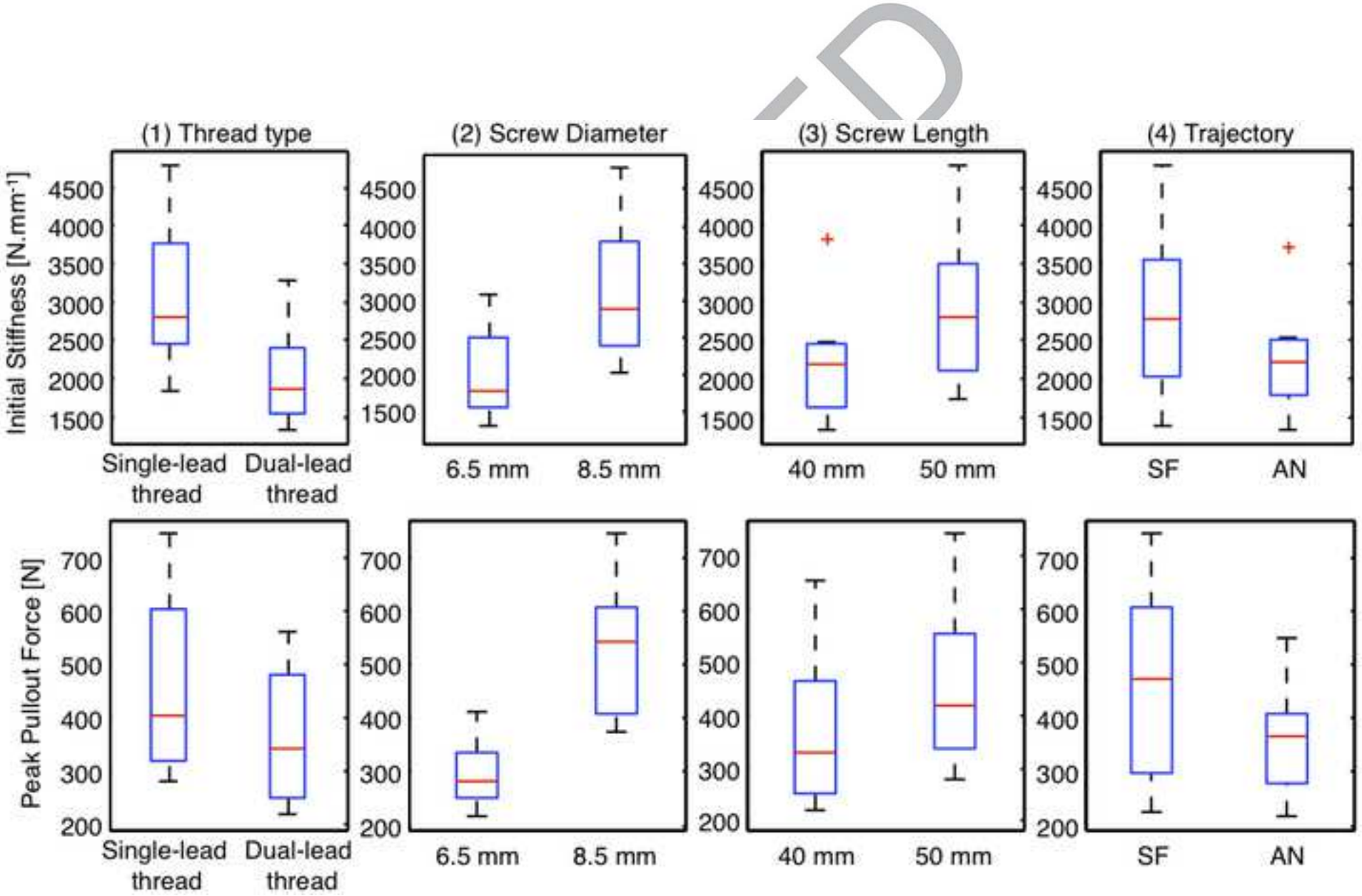

Copyright © Lippincott Williams & Wilkins. Unauthorized reproduction of the article is prohibited.